NeuroToxicology 59 (2017) 88–97

Contents lists available at ScienceDirect

NeuroToxicology

Full Length Article

27-Hydroxycholesterol regulates cholesterol synthesis and transport in C6 glioma cells

Yu An[a,1], Dan-Di Zhang[a,b,1], Huan-Ling Yu[a], Wei-Wei Ma[a], Yan-Hui Lu[a], Quan-Ri Liu[a], Rong Xiao[a,*]

[a] School of Public Health, Beijing Key Laboratory of Environmental Toxicology, Capital Medical University, Beijing 100069, China
[b] Department of Nutrition, Beijing Luhe Hospital Affiliated to Capital Medical University, Beijing 101149, China

ARTICLE INFO

Article history:
Received 30 May 2016
Received in revised form 1 February 2017
Accepted 2 February 2017
Available online 3 February 2017

Keywords:
27-hydroxycholesterol
Cholesterol
Synthesis
Transport
Brain
Astrocyte

ABSTRACT

The oxysterol 27-Hydroxycholesterol (27-OHC) is a major cholesterol metabolite that can cross the blood brain barrier (BBB) from peripheral circulation to the brain. Currently, the role of 27-OHC on cholesterol homeostasis in astrocytes and the underlying mechanisms are not defined. Since all brain cholesterol is essentially synthesized in brain itself and astrocytes as net producers of cholesterol are essential for normal brain function, here we investigated the effects of 27-OHC on cholesterol synthesis and transport in C6 glioma cells. C6 cells were treated with 5, 10 and 20 μM 27-OHC for 24 h and the cell viability and apoptosis, the cholesterol levels and metabolism-related mediators, genes and proteins were subsequently assessed using cell-counting kit (CCK)-8, Amplex red, ELISA, real-time PCR and Western blot, respectively. We found that 27-OHC decreased cholesterol levels by down-regulating the expression of sterol-regulated element binding protein-1 (SREBP-1a), 3-hydroxy-3-methylglutaryl-CoA reductase (HMG-CR) and low density lipoprotein receptor (LDLR) and promoted cholesterol transport by up-regulating the expression of peroxisome proliferator-activated receptors-γ (PPAR-γ), liver X receptor-α (LXR-α), ATP-binding cassette transporter protein family member A1 (ABCA1) and apolipoprotein E (ApoE)genes. Our results suggested that 27-OHC may represent a sensitive modulator of cholesterol metabolism disorder by suppressing cholesterol synthesis and stimulating cholesterol transport in astrocytes.

1. Introduction

Disturbances in brain cholesterol homeostasis may lead to learning and memory deficits and even to neurodegenerative diseases such as Alzheimer's disease (AD) (Di Paolo and Kim, 2011). Some studies have indicated that high levels of brain cholesterol are responsible for β-amyloid peptide (Aβ) accumulation in AD patients and dysfunctional cholesterol metabolism may increase the risk of developing AD (Nicholson and Ferreira, 2010). Despite lack of conclusive evidence, a substantial body of literature supports the contention that high levels of plasma cholesterol can also influence the pathogenesis of AD (Kivipelto et al., 2001; Refolo et al., 2000; Solomon et al., 2009). However, the question as to how plasma cholesterol contributes to the development of AD remains to be answered in view of the fact that the brain makes its own cholesterol in situ and little or no circulating cholesterol enters into the brain owing to the impermeability of the blood brain barrier (BBB) (Pfrieger and Ungerer, 2011). At the present state of knowledge, several hypotheses have been advanced to explain the question and it may be possible that oxysterols, side-chain oxidized metabolites of cholesterol, may represent the link between circulating cholesterol and the development of AD.

In marked contrast to cholesterol, oxysterols have the ability to cross the BBB into the brain. One of these metabolites, 27-hydroxycholesterol (27-OHC), is the quantitatively most important cholesterol metabolite originating mainly from the peripheral circulation and is formed by the mitochondrial cytochrome P450 sterol 27-hydroxylase (CYP27A1) enzyme (Marwarha and Ghribi, 2014). Heverin et al. have reported a substantial continuous flux of 27-OHC from the circulation into the brain and the levels of 27-OHC in cerebrospinal fluid (CSF) are associated with the corresponding levels in periphery (Heverin et al., 2005), indicating the correlation between hypercholesterolemia and increased flux

* Corresponding author at: School of Public Health, Beijing Key Laboratory of Environmental Toxicology, Capital Medical University, No.10 Xitoutiao, You An Men Wai, Beijing 100069, China.
E-mail address: xiaor22@ccmu.edu.cn (R. Xiao).
[1] These authors contributed equally to the work.

http://dx.doi.org/10.1016/j.neuro.2017.02.001
0161-813X/

of 27-OHC into the brain. The levels of 27-OHC have been demonstrated a significant increase in AD brains (Heverin et al., 2004). On the other hand, the oxysterol 24S-hydroxycholesterol (24-OHC), which is also involved in the pathogenesis of AD, is synthesized in neurons from cholesterol by CYP46A1 enzyme that is expressed exclusively in the brain (Hughes et al., 2013).

Currently, the role of these two oxysterols and the mechanism by which they are important to the pathogenesis of AD have not been clearly defined. Under in vitro conditions, 27-OHC was reported to enhance production of β amyloid (Aβ) in human neuroblastoma SH-SY5Y cells and 24-OHC may favor the non-amyloidogenic pathway (Prasanthi et al., 2009). In addition, our team has also shown that 27-OHC may represent a pathogenic factor in AD by regulating Nrf2 signaling pathway and increasing oxidative stress in astrocyte cells (Ma et al., 2015). These studies have revealed some potential mechanism. However, it has been reported that oxysterols have diverse physiological and biochemical functions, including maintaining cholesterol homeostasis and regulating nuclear receptors (Javitt, 2007). Within the mature brain, astrocytes, in particular, synthesize and release cholesterol (Pfrieger, 2003). Oxysterols can suppress cholesterol synthesis in response to high levels of cholesterol by interacting with the absence of activated sterol regulatory element-binding proteins (SREBPs) and degradation of the 3-hydroxy-3-methylglutaryl coenzyme A reductase (HMG-CR). Besides, oxysterols can also bind liver X receptor (LXR) and then affect the expression of several genes involved in cholesterol metabolism (Leoni and Caccia, 2013). Excessive formation of 27-OHC followed by hypercholesterolemia may contribute to disturbances in brain cholesterol homeostasis and subsequently pathogenesis of AD. Although evidence has provided that 24S-OHC induces cholesterol efflux via an LXR-controlled pathway in astrocytes, which may be relevant for neurological diseases (Abildayeva et al., 2006), it remains less understood that whether 27-OHC may induce similar disruptive brain cholesterol homeostasis in astrocyte cells.

In this study we tested the hypothesis that 27-OHC contributes to the disruptive cholesterol homeostasis in astrocytes. For this purpose the effects of 27-OHC on cholesterol metabolism in C6 glioma cells were detected. The levels of total cholesterol (TC), free cholesterol (FC) and cholesterol esterase (CE), as well as the mRNA and protein of HMG-CoA reductase (HMG-CR), sterol regulatory element-binding protein-1a (SREBP-1a), low-density lipoprotein receptor (LDLR), peroxisome proliferator-activated receptor-γ (PPAR-γ), liver X receptor-α (LXR-α), ATP-binding cassette transporter protein family member A1(ABCA1) and apolipoprotein E (ApoE) in C6 cells treated with 27-OHC were especially determined. Additionally, cell viability and apoptosis assays were also performed to assess the cytotoxicity of 27-OHC; ELISA assay kits were used for evaluation of HMG-CR, low-density lipoprotein (LDL), cholesterol ester transfer protein (CETP) and microsomal triglyceride transfer protein (MTTP).

2. Materials and methods

2.1. Materials and cell lines

The C6 rat glioma cell line was obtained from Peking Union Medical Center Laboratory, Beijing, China. 27-OHC was purchased from Santa Cruz Biotechnology Company (USA). The stock solution was prepared by dissolving 27-OHC in ethanol to 1000 μM and stored at −80 °C until use. Before each cell treatment, 27-OHC was first diluted in saline with 8% ethanol (v/v) and then added to culture medium to a final concentration of 5, 10 and 20 μM, containing 0.04%, 0.08% and 0.16% ethanol (v/v). DMEM, fetal bovine serum (FBS) and penicillin (10,000 units/ml)/streptomycin (10,000 μg/mL) (P/S) were purchased from Gibco Biotechnology Company (USA). The study design has been approved by the Ethics Committee of Capital Medical University (AEEI-2014-047).

2.2. Cell culture

The C6 cells were cultured in DMEM supplemented with FBS (10%) and penicillin (100 U/ml)/streptomycin (100 U/ml) at 37 °C in an atmosphere of CO_2 (5%)/air (95%). The cells were seeded at an appropriate density (1×10^6 cells/cm^2) in culture dishes. The culture medium was replaced every 2 days. Cells incubated with DMEM were used as control group and others were treated with 5, 10, and 20 μM 27-OHC for 24 h.

2.3. CCK-8 assay kit

The 2-(2-methoxy-4-nitrophenyl)-3-(4-nitrophenyl)-5-(2,4-disulfophenyl)-2H-tetrazolium sodium salt (WST-8/CCK-8) assay was used to measure cell viability. Briefly, C6 cells were seeded at 5×10^4 cells/ml (150 μl per well) in 96-well plates for 24 h in DMEM. Then, the cells were incubated with 0 μM, 1 μM, 3 μM, 10 μM, 30 μM, 100 μM, or 300 μM 27-OHC for 24 h. After treatment with 27-OHC for 24 h, CCK-8 reagent (10 μl) in DMEM (100 μl) was added to each well, and the cultures were incubated at 37 °C for 4 h. The absorbance was measured with a microplate reader (Tecan, Switzerland) at a wavelength of 450 nm.

2.4. Annexin V-FITC/PI assay kit

C6 cells were treated with increasing concentrations of 27-OHC (0 μM, 1 μM, 3 μM, 10 μM, 30 μM, 100 μM) for 24 h, washed with PBS and trypsination. The apoptosis was detected with Annexin V-FITC/propidium iodine (PI), according to the guidelines of assay kit (Beijing Keygen Biotech, China). Laser excitation wavelength was 488 nm, the green signal from Annexin V-FITC was examined at 525 nm and the red signal from PI was measured at 620 nm. Annexin V^-/PI^- cells are vitality; Annexin V^+/PI^- cells are in early apoptosis; Annexin V^+/PI^+ cells are necrotic or in late apoptosis. Each sample was set up in triplicate within the assay, and at least three independent experiments were performed.

2.5. Amplex red cholesterol assay

The cholesterol content in the C6 cells was tested using the Amplex Red Cholesterol Assay kit (Invitrogen) according to the manufacturer's instructions. Briefly, the C6 cells were seeded at density of 1×10^6cells/cm^2 in culture dishes. After 24 h incubation of 27-OHC at 37 °C in a CO2 (5%)/air (95%) atmosphere, sub-confluent cultures were rinsed three times in PBS to eliminate residual growth medium. Whole cell extracts were prepared by 0.5 ml RIPA lysis buffer (0.5% sodium deoxycholate, 0.1%SDS, 1% NP-40, 150 mM NaCl, 1 mM DTT, 50 mM Tris–HCl (pH 7.4) and phenylmethanesulfonyl fluoride (PMSF). After vigorous shaking for 40 min at 4 °C, lysates were clarified at 15,000 g for 20 min at 4 °C and supernatants containing protein were evaluated using BSA as a standard for protein concentration by BCA assay. Cell extracts were diluted with 1 × cholesterol reaction buffer (0.1 M potassium phosphate, pH 7.4, 0.05 M NaCl, 5 mM cholic acid, and 0.1% Triton X-100). Then, 50 μl of 150 μM Amplex Red reagent (1 U/ml horseradish peroxidase, 1 U/ml cholesterol oxidase, and 1 U/ml cholesterol esterase) was added to 50 μl samples in 96-well plates. After a 60-min incubation at 37 °C in the dark, the sample fluorescence was measured using a microplate reader (Tecan, Switzerland) at 530/25 nm excitation and 590/35 nm emission wavelengths. The total cholesterol (TC) content was determined by measuring the cholesterol concentration following digestion with cholesterol esterase (CE). To measure the free cholesterol (FC), CE

was omitted from the assay. Each sample was set up in triplicate within the assay, and at least three independent experiments were performed. The values obtained from a cholesterol standard curve were normalized.

2.6. Filipin III assay

The cholesterol in the C6 cells was stained using the Filipin III Assay kit (Abcam, USA) according to the manufacturer's instructions. The C6 cells at a concentration of 1×10^4/mL were cultured on 22 mm × 22 mm coverslips in 6-well plates overnight. Then, the cells were treated with 5 μM, 10 μM, 20 μM 27-OHC for 24 h. Cells were washed with PBS and fixed with 4% formaldehyde in PBS for 30 min at 4 °C. They were subsequently treated with 0.1% Triton for 3 min, and washed three times with PBS. Cells were stained with 50 μg/mL Filipin III fluorescent dye at 37 °C for 30 min and washed with PBS three times. Images were obtained with a fluorescent microscope (Leica).

2.7. ELISA assay

Detection of HMG-CR, **LDL receptor**, MTTP and CETP in the cell lysates of treated and untreated C6 cells were measured with rat Enzyme-linked Immunosorbent Assay kits (Cloud-Clone Corp., China) according to the manufacturer's instructions. Briefly, the cells were detached with trypsin and then collected by centrifugation. Resuspend cells in ice-cold PBS (phosphate-buffered saline; 0.01 mol/L, pH 7.0–7.2) and the cells were subject to ultrasonication, then centrifuged for 10 min at 1500 × *g*. One hundred microliters of the resulting suspension were added to a 96-well plate coated with the appropriate purified **antibody** and incubated for 2 h at 37 °C. The absorption was subsequently measured at 450 nm using a microplate reader (Tecan, Switzerland). The mean and standard errors of the repeated (at least three) measurements were calculated for each tested sample.

2.8. Real time polymerase chain reaction (real-time PCR)

The mRNA of the C6 cells was purified using the SV Total RNA Isolation system (Promega Corporation, Madison, WI, USA). The mRNA expression levels of HMG-CR, SREBP-1a, LXR-α, ABCA1, ApoE (invariant Control) were analyzed by real-time PCR. Reverse transcription (RT) was performed with a Reverse Transcription System (Promega Corporation Madison, WI, USA). Briefly, double-stranded DNA was synthesized from 1 μg of total RNA and used as a template for the real time polymerase chain reaction (real-time PCR). The forward and reverse sequences of the primers are shown in Table 1. The real-time PCR system included 0.5 μl of forward primer (50 μM solution), 0.5 μl of reverse primer (50 μM solution), 10 μl of SYBR Green PCR Master Mix (Applied Biosystems), 8 μl of nucleus-free water and 1 μl of cDNA, for a total volume of 20 μl in each well. Care was taken to avoid cross contamination of the samples. The reaction plate was covered with an adhesive cover. Real-time PCR experiments were performed on a CFX Connect Real-Time PCR Detection System (Bio-Rad, Germany) as follows: 50 °C for 2 min, an initial denaturation at 95 °C for 10 min, and 40 cycles including strand separation at 95 °C for 15 s; the housekeeping gene 18S rRNA served as the reference for standardization. All of the measurements were performed in duplicate, and the experiment was repeated once. Fold changes were calculated using the ΔC_t (C_t of the target gene-C_t of the housekeeping gene) method where the fold change is equal to $2^{-\Delta Ct}$ for the gene analysis level.

Table 1
Primer sets for real-time RT-PCR analysis of gene expression.

Primer	Forward sequence(5′-3′)	Reverse sequence(5′-3′)	Tm/◦C
18srRNA	AAACGGCTACCACATCCA	CTCATTCCAATTACAGGG	48
HMGCR	TGTTCACGCTCACAGTCG	TGGAGAGGTAAAACTGCC	50
SREBP-1a	GACAAACTGCCCATCCAC	TCAGCTTTGCCTCAGTGC	51
LDLR	GTAAACTGGTGTGAGGCAAC	TAGCATACCATCAGGGCAAG	60
CYP46A1	GCCGACATCCTCACGCAGATTC	AACCGACCACCTCATCCACCTC	59
PPAR-γ	CGTTCACAAGAGCTGACC	CCATGAGGGAGTTTGAAG	50
LXR-α	CTTGCTGAAGACCTCTGC	GGAGAACTCAAAGATGGG	50
LXR-β	ACCTGCCAGATGGATGCCTTCA	GCTGCTGCTGTTGCTGCTTCT	57
ABCA1	ATTTGGAAGGCACTCAAG	CCAGGTCAGGGAACAAAG	49
ApoE	AACCGCTTCTGGGATTAC	GTGTCTCCTCCGCCACTG	57

2.9. Western Blot analysis

The treated C6 cells were washed with phosphate-buffered saline (PBS), trypsinized to collect the cells and centrifuged at 800*g* for 5 min. The C6 sediments were lysed for 40 min at 4 °C by vigorous shaking in radioimmunoprecipitation assay (RIPA) buffer, and protease inhibitors and then centrifuged again at 12,000*g* for 20 min. The supernatant containing the protein was collected for further analysis. The protein concentration was then detected using a bicinchoninic acid (BCA) protein assay kit (Pierce Biotechnology, USA). Protein samples (50 μg) were loaded on 6% or 10% SDS-acrylamide gels for separation by electrophoresis and then transferred to polyvinylidene fluoride membranes at a voltage of 120 V for 30 min and 80 V for 2 h. The transferred membranes were blocked using fresh 5% nonfat dry milk dissolved in Tris-buffered saline Tween-20 (TBST) at room temperature for 1 h. Immunoblots were probed with appropriate antibodies. The primary anti-SREBP-1a (1:800), anti-ApoE (1:1000), anti-Actin (1:1000), anti-PPAR-γ (1:800) and anti-LXR-α (1:800) antibodies were purchased from Cell Signaling Technology, and anti-HMG-CR (1:1000), anti-LDLR (1:1000) and anti-ABCA1 (1:600) were purchased from Abcam (USA). Each primary antibody was individually incubated with the membrane at 4 °C for 12 h. After completing the primary antibody incubation and washing with TBST three times, the membranes were incubated for 1 h with the appropriate secondary antibody (diluted 1:2000 in TBST) and finally washed again three times with TBST. The membranes were covered with 1 ml of enhanced chemiluminescence (ECL) (Promega) Plus substrate for 2 min and then placed in a sealed bag. The membranes were scanned using a Kodak Image Station, and the gray values were then analyzed. Each experiment was repeated at least three times.

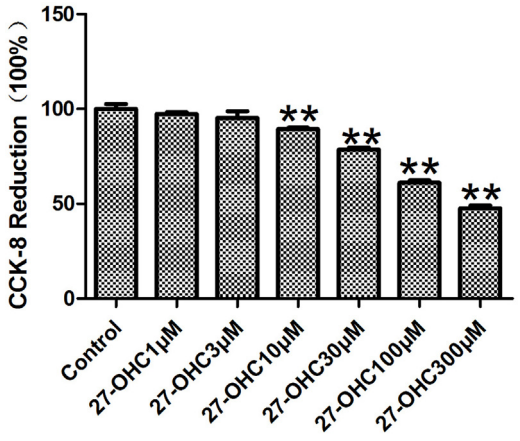

Fig 1. The cell viability of C6 cells from untreated control group to exposed to different doses of 1, 3, 10, 30, 100, 300 μM 27-OHC groups. All the data were shown as mean ± SE. *: $P < 0.05$ compared with Control group, **: $P < 0.01$ compared with Control group.

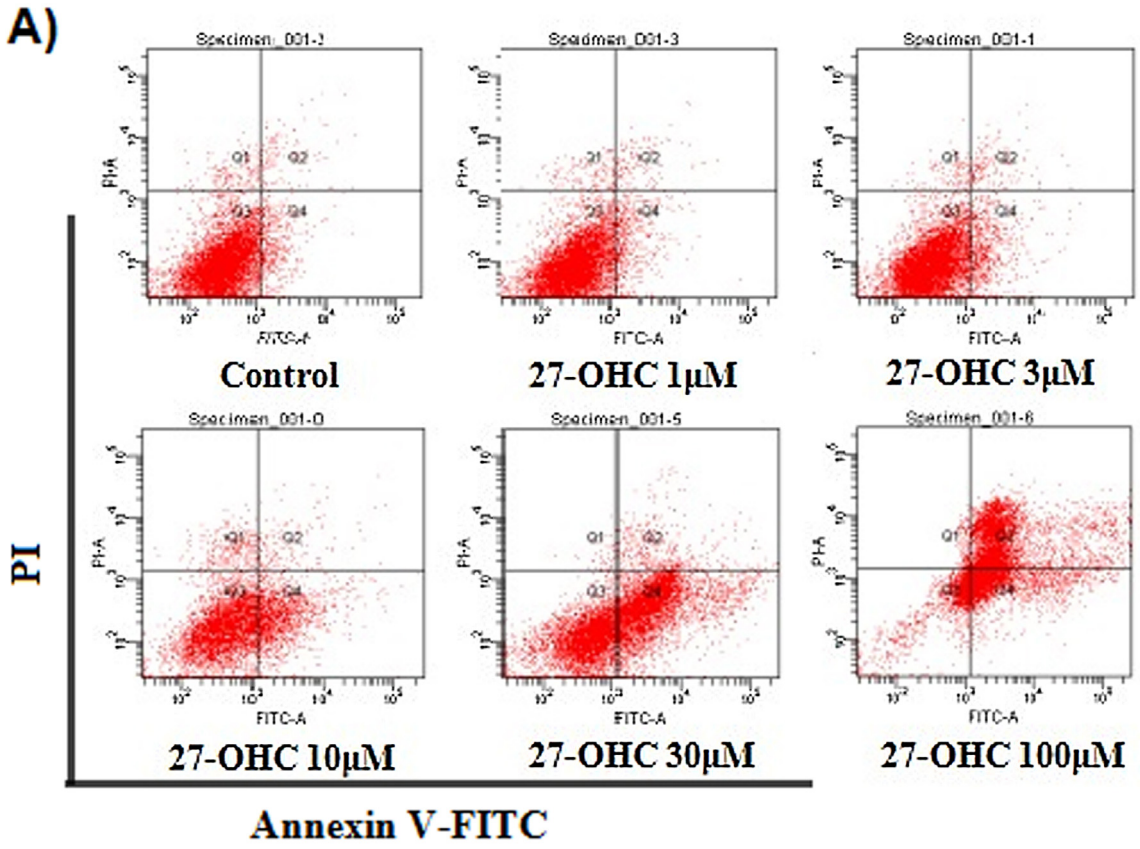

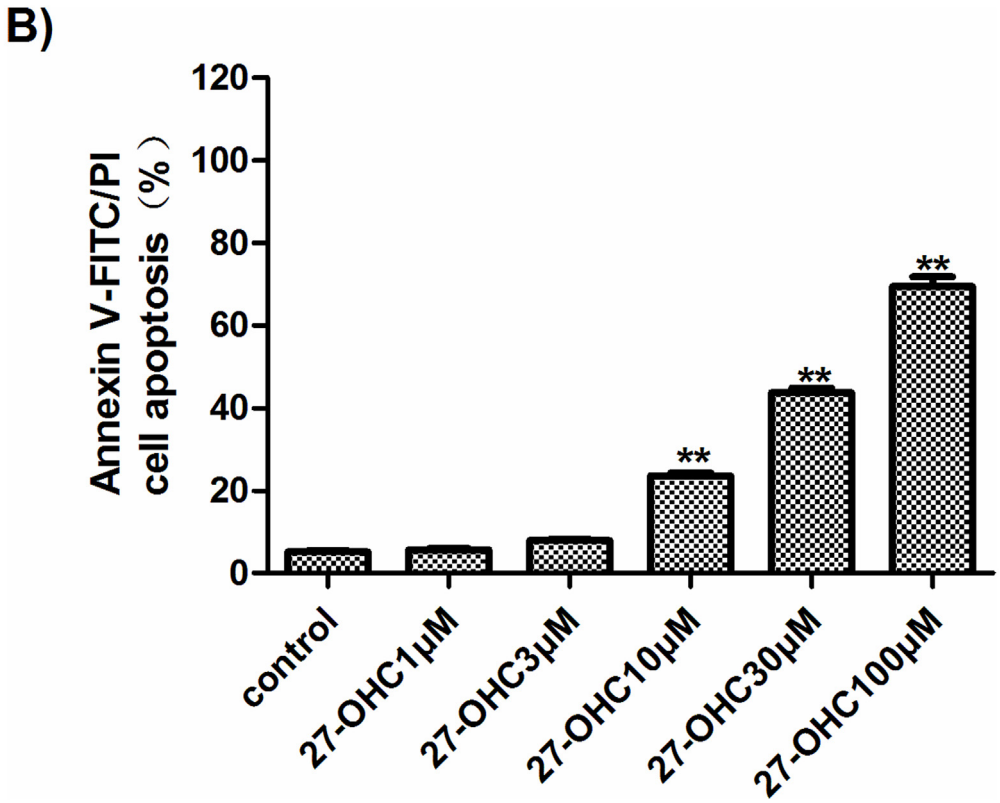

Fig. 2. The cell apoptosis of C6 cells from untreated control group to exposed to different doses of 1, 3, 10, 30, 100 μM 27-OHC groups. A) The fluorescence intensity of Annexin V-FITC/PI in C6 cells; B) The average flourescence intensity of C6 cells. All the data were shown as mean ± SE. *: $P < 0.05$ compared with Control group, **: $P < 0.01$ compared with Control group.

2.10. Statistical analysis

All of the data are expressed as the mean ± standard error (SE). Differences between the groups were compared with Statistical Package for Social Science (SPSS) 17.0 (SPSS Inc., Chicago, America) using one-way analysis of variance (ANOVA) and post hoc comparisons were evaluated using the LSD tests. All of the statistical tests were 2-sided, and a significant level was set at $p < 0.05$.

3. Results

3.1. Effects of 27-OHC on cell viability in C6 cells

To determine the toxic effect of 27-OHC, the viability of the C6 cells was measured based on a CCK-8 assay. Compared with the Control group, the cell viability was significantly decreased after treatment with 10 μM and more than 10 μM 27-OHC ($F = 9.759$, $p < 0.001$). Because of the toxic effect of 27-OHC on the C6 cells, a concentration of 10 μM 27-OHC was selected to incubate the C6 cells for 24 h (Fig. 1).

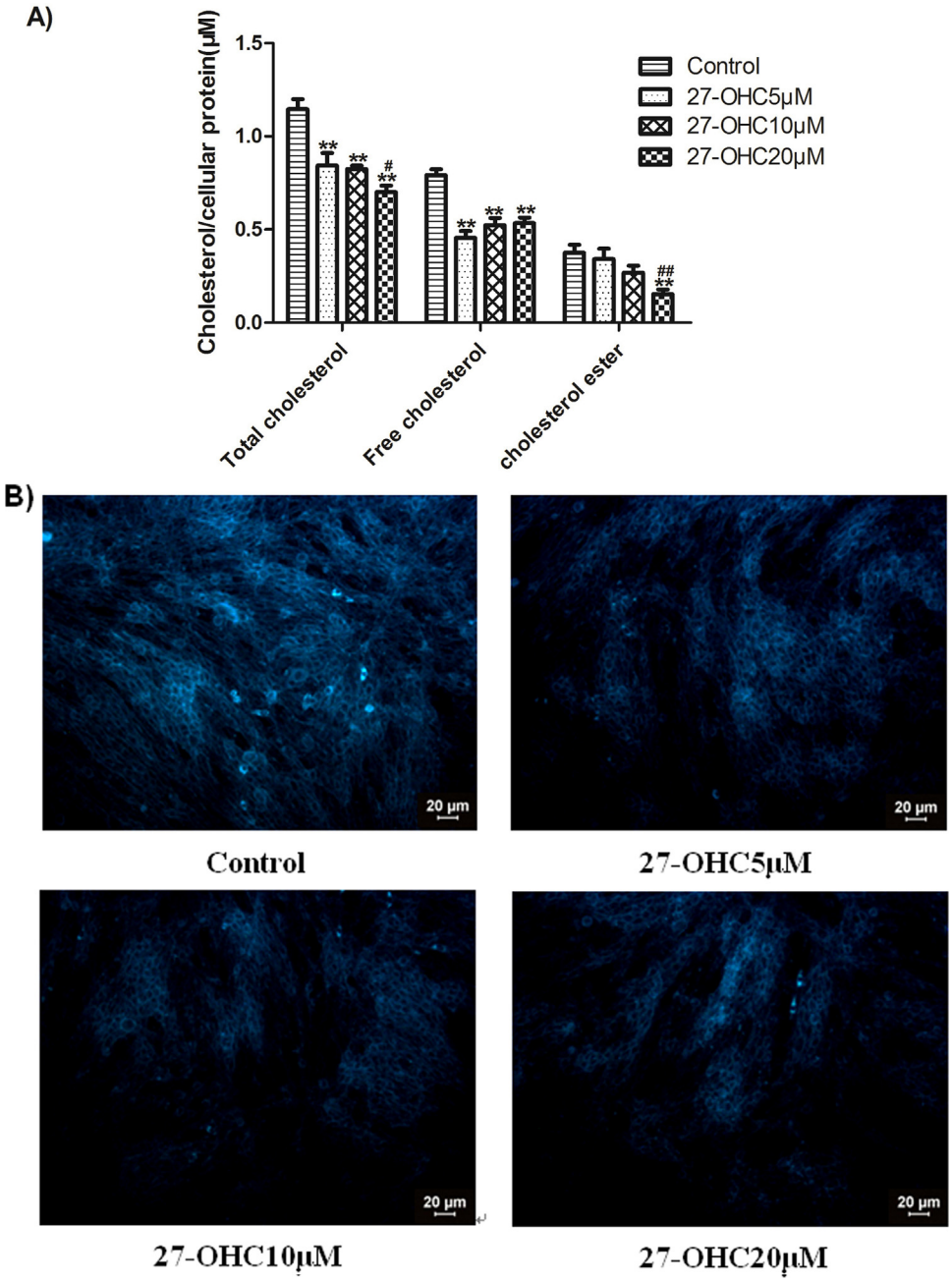

Fig. 3. The total cholesterol, free choletrol and cholesterol ester of celluler protein in C6 cells treated with 5, 10 and 20 μM 27-OHC (A). All the data were shown as mean ± SE. *: $P < 0.05$ compared with control group; **: $P < 0.01$ compared with control group. *: $P < 0.05$ compared with control group; **: $P < 0.01$ compared with control group; #: $p < 0.05$ compared with 27-OHC5 μM group; ##: $p < 0.01$ compared with 27-OHC5 μM group. &: $p < 0.05$ compared with 27-OHC10 μM group; &&: $p < 0.01$ compared with 27-OHC10 μM group. The morphological shapes of cholesterol in 27-OHC treated with C6 glioma cells were stained with filipin (B).

3.2. Effects of 27-OHC on cell apoptosis in C6 cells

C6 cells were treated with different concentration of 27-OHC and analyzed for Annexin V-FITC/PI assay kit (Fig. 2). The results showed that 27-OHC induced apoptosis in C6 cells **($F = 54.551$, $p < 0.001$)**. 27-OHC at a concentration of 10 μM was found to induce early and late apoptosis to 23.6% of cells, and at higher concentration of 30 μM and 100 μM, the percentage of apoptotic cells increased up to 43.7% and 69.3%, respectively.

3.3. Effects of 27-OHC on cholesterol content in C6 glioma cells

The Amplex Red Cholesterol Assay kit for TC, FC and CE quantification showed that the C6 cells expressed basal levels of cholesterol. The TC ($F = 15.728$, $p < 0.001$), FC ($F = 18.267$, $p < 0.001$) and CE ($F = 5.513$, $p = 0.006$) levels of cellular protein from the C6 cells treated with 5, 10 and 20 μM 27-OHC was significantly decreased compared with Control. Our results showed that 27-OHC decreased the levels of TC and FC (Fig. 3A), suggesting that 27-OHC might be an efficient regulator of cholesterol metabolism in vitro. Besides, images from fluorescent microscope showed that 27-OHC at increasing concentration loading in C6 cells caused significantly decreased cholesterol, observed as blue staining of morphological shapes of cholesterol by filipin (Fig. 3B).

3.4. Effects of 27-OHC on HMG-CR, LDL, MTTP and CETP in C6 glioma cells

Compared with Control group, 27-OHC remarkably down-regulated the levels of HMG-CR ($F = 5.925$, $p = 0.006$), LDL ($F = 5.875$, $p = 0.005$), MTTP ($F = 4.347$, $p = 0.027$) and CETP ($F = 5.843$, $p = 0.007$) in the C6 cells of 10 and 20 μM groups. However, no significant difference was observed between the 5 μM group and the Control group (Fig. 4).

3.5. Effects of 27-OHC on cholesterol synthesis in C6 glioma cells

As shown in Fig. 5, treatment with 5, 10 and 20 μM of 27-OHC remarkably down-regulated the levels of mRNA and protein of HMG-CR ($F = 51.588$, $p < 0.001$; $F = 8.607$, $p < 0.001$). Levels of mRNA and protein of SREBP-1a ($F = 18.310$, $p = 0.001$; $F = 15.636$, $p < 0.001$)and LDLR ($F = 5.966$, $p = 0.019$; $F = 2.925$, $p = 0.066$) increased in 27-OHC 10 and 20 μM groups compared with the Control group; no significant differences of mRNA and protein levels were observed between the 5 μM group and the Control group. These results suggest that 27-OHC might be an efficient suppressor of cholesterol synthesis in C6 cells and is implicated in the inhibition of the rate-limiting enzyme HMG-CR or the inhibition of SREBP-1a and LDLR.

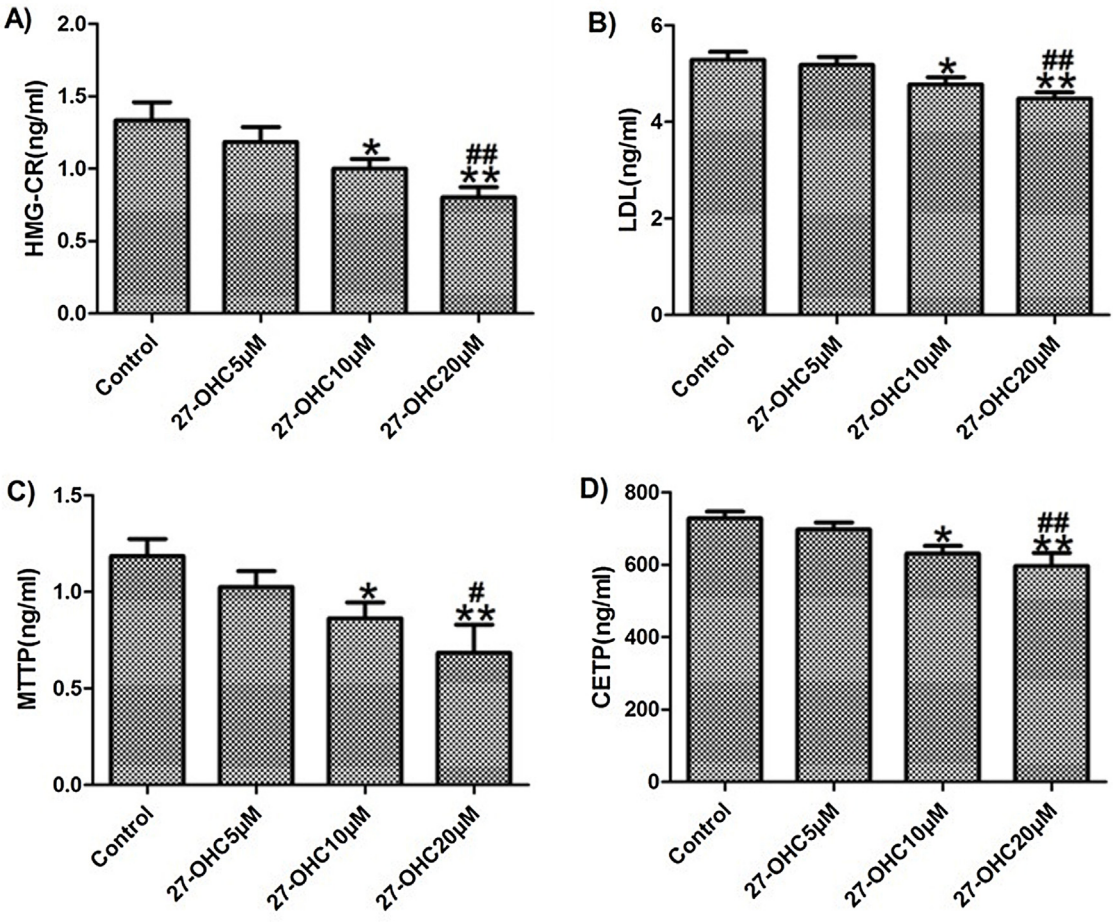

Fig. 4. The levels of 3-hydroxy −3-methylglutaryl-CoA reductase (HMG-CR) A), low density lipoprotein receptor (LDL) B), microsomal triglyceride transfer protein (MTTP) C) and Cholesterol ester transfer protein (CETP) D) from C6 cells treated with 5, 10 and 20 μM 27-OHC. All the data were shown as mean ± SE. *: $P < 0.05$ compared with control group; **: $P < 0.01$ compared with control group. #: $p < 0.05$ compared with 27-OHC5 μM group; ##: $p < 0.01$ compared with 27-OHC5 μM group. &: $p < 0.05$ compared with 27-OHC10 μM group; &&: $p < 0.01$ compared with 27-OHC10 μM group.

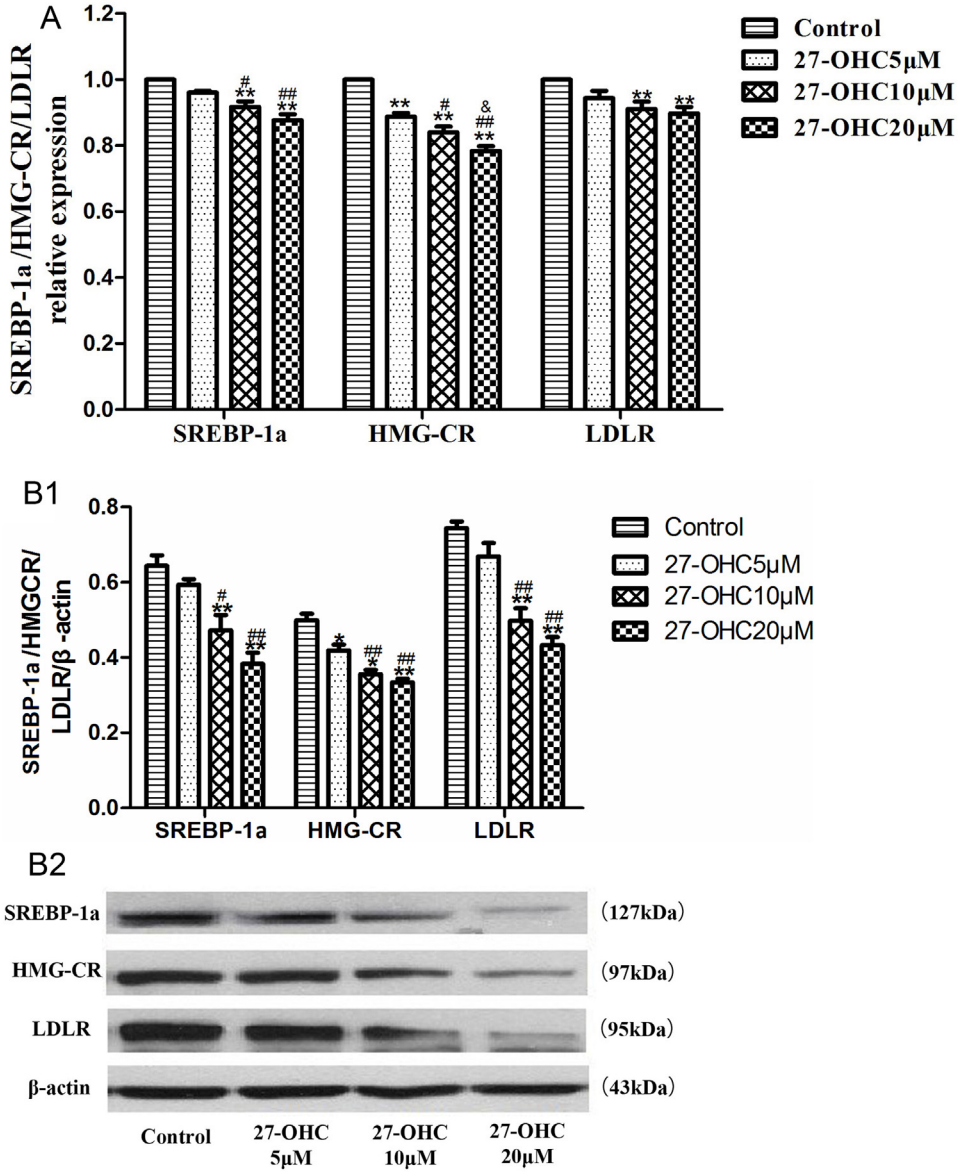

Fig. 5. The mRNA (A) and protein (B) expression of SREBP-1a, HMG-CR and LDLR in C6 cells treated with 5, 10 and 20 μM 27-OHC. All the data were shown as mean ± SE. *: $P < 0.05$ compared with control group; **: $P < 0.01$ compared with control group. #: $p < 0.05$ compared with 27-OHC5 μM group; ##: $p < 0.01$ compared with 27-OHC5 μM group. &: $p < 0.05$ compared with 27-OHC10 μM group; &&: $p < 0.01$ compared with 27-OHC10 μM group.

3.6. Effects of 27-OHC on cholesterol transport in C6 glioma cells

Compared with the Control group, treatment with 5, 10 and 20 μM of 27-OHC significantly increased the mRNA levels of LXR-α ($F = 5.776$, $p = 0.021$, Fig. 6A), and up-regulated PPAR-γ ($F = 5.497$, $p = 0.024$), ABCA1 ($F = 3.710$, $p = 0.023$) and ApoE ($F = 5.048$, $p = 0.017$) protein levels (Fig. 6B). Meanwhile, there was a significant increase in the mRNA levels of ABCA1 ($F = 4.899$, $p = 0.032$), ApoE ($F = 81.782$, $p < 0.001$) and PPAR-γ ($F = 11.350$, $p = 0.003$), and the protein levels of LXR-α ($F = 11.017$, $p < 0.001$) in the 10 and 20 μM groups (Fig. 6A). However, the protein levels of LXR-α, the mRNA levels of PPAR-γ, ABCA1and ApoE in the 5 μM group were not found significant difference but an increasing trend compared with the Control group (Fig. 6).

4. Discussion

Accumulating evidence has indicated a link between cholesterol metabolism and neurodegenerative diseases. Hypercholesterolemia has been considered one of risk factors for Alzheimer's disease (Bjorkhem et al., 2009). The failure to manifest a transfer of cholesterol from periphery into the brain makes it difficult to explain the link. Contrary to cholesterol itself, oxysterols, sidechain oxidized cholesterol metabolites, have the ability to pass the BBB (Wang et al., 2016). 27-OHC is quantitatively the most important oxysterol in the peripheral circulation and correlated with the levels of cholesterol. Different groups measuring circulating 27-OHC levels in human have yielded comparatively consistent values, generally between 0.15 and 0.73 μM (Brown and Jessup, 1999) and 27-OHC is imported to brain at a rate of about 4–5 mg/24 h (Iuliano et al., 2015). In spite of the substantial flux of 27-OHC, the brain levels of 27-OHC are relatively low, suggesting a very active metabolism of 27-OHC, and 7-hydroxy-3-oxo-4-cholestenoic acid (7-HOCA) has reported to be the major end metabolite (Saeed et al., 2014).

Recent research has shown patients with AD have increased levels of 27-OHC in brain. The level of 27-OHC in formalin-fixed autopsy brain tissue including the frontal cortex, occipital cortex,

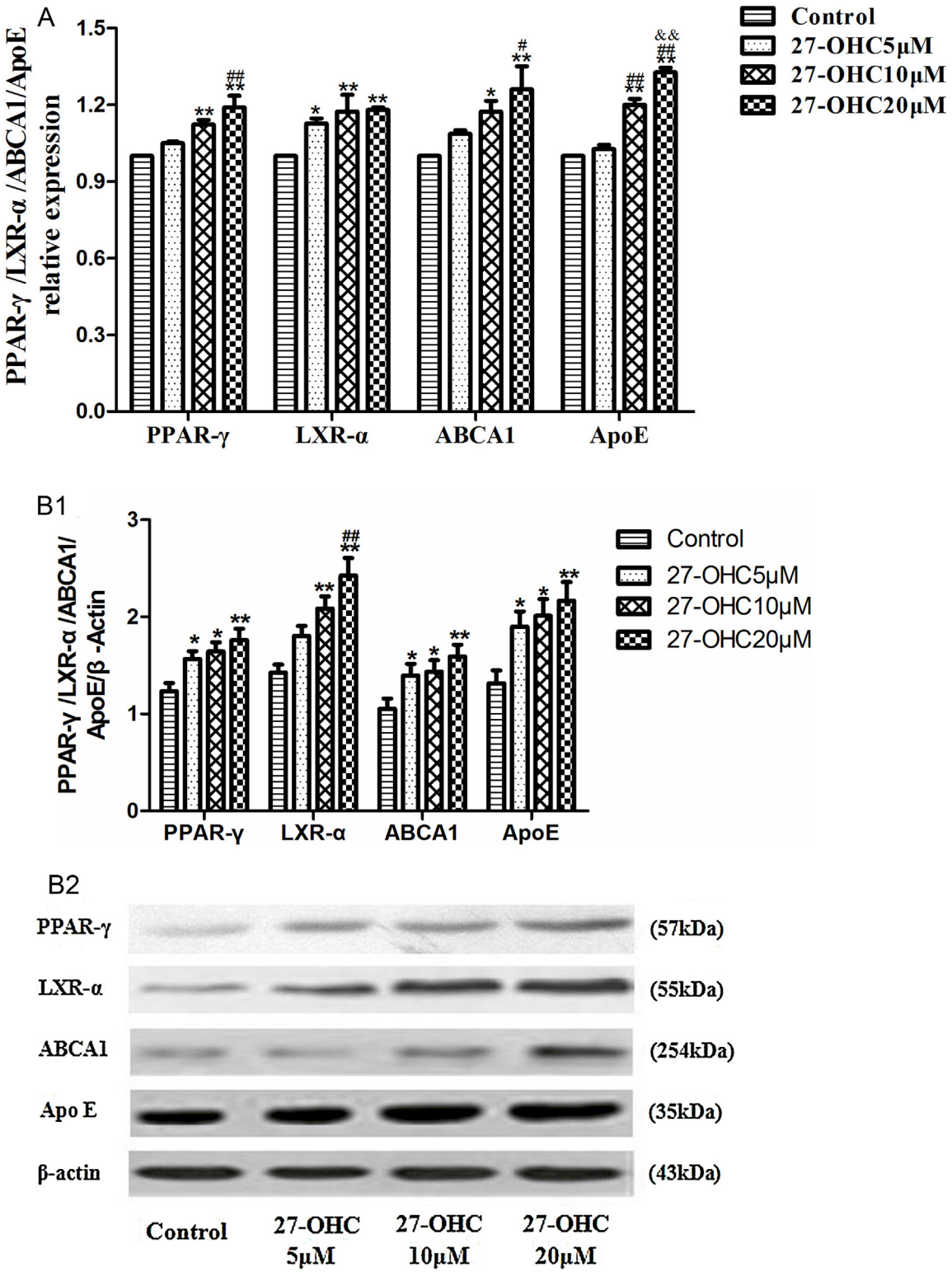

Fig. 6. The mRNA (A) and protein (B) expression of PPAR-γ, LXR-α, ABCA1, ApoE in C6 cells treated with 5, 10 and 20 μM 27-OHC. All the data were shown as mean ± SE. *: $P < 0.05$ compared with control group; **: $P < 0.01$ compared with control group. #: $p < 0.05$ compared with 27-OHC5 μM group; ##: $p < 0.01$ compared with 27-OHC5 μM group. &: $p < 0.05$ compared with 27-OHC10 μM group; &&: $p < 0.01$ compared with 27-OHC10 μM group.

basal ganglia from elderly AD patients and matched controls (age 61–92 years) is about 1–6 ng/mg (Heverin et al., 2004) and 27-OHC levels are significantly higher in neuropathological situations. Altered cholesterol metabolism has been reported to play important roles in AD-like pathology (Gamba et al., 2012). Our previous study has demonstrated that excessive 27-OHC with concentrations of 7, 21 and 70 μM in blood impairs spatial learning and memory and contributes to the perturbation of brain cholesterol metabolism in the rat brain (Zhang et al., 2015). Furthermore, treatment with concentration of 5, 10, 20 μM 27-OHC, higher than the typical physiological concentration, on C6 glioma cells in the present study were undertaken to further shed

light on the mechanism by which influx of 27-OHC into the brain contributes to the disruption of cholesterol homeostasis.

We have found that 27-OHC provided a feedback control of cholesterol synthesis since 27-OHC significantly reduced SREBP-1a, HMG-CR and LDLR expression in C6 glioma cells. Concomitantly, C6 cells treated with 27-OHC reduced their cellular cholesterol content (TC, FC and CE)and the concentrations of HMG-CR, LDL, MTTP and CETP compared with the control ($p < 0.05$).

The rate limiting enzyme of cholesterol production is HMG-CR. The supply of cholesterol is regulated by the LDL receptor (LDLR) via the uptake of LDL. The transcription of genes encoding HMG-CR and LDLR are regulated at different rate according to the cholesterol levels in cells. Genes encoding the LDL receptor and HMG-CR were both identified SREBP-regulated ones (Horton et al., 2002). SREBPs is a family of membrane bound transcription factors that regulate cholesterol homeostasis and activate the expression of some genes involved in the synthesis of cholesterol. SREBPs exist in three forms comprising SREBP-2 primarily involved in cholesterol synthesis, SREBP-1c primarily stimulating fatty acid synthesis and SREBP-1a preferably activating cholesterol synthesis (Wang et al., 2008). SREBP-1a and SREBP-1c are derived from the same gene but transcribed through the use of alternative transcription start sites, thus leading to the difference in their first exon (exon 1a and exon 1c) (Eberle et al., 2004). There has been evidence that 27-OHC is an intracellular mediator between inhibition of low-density lipoprotein (LDL) uptake and the degradation and suppression of HMG-CR in cell lines in a concentration-dependent manner (Axelson and Larsson, 1995; Bellosta et al., 1993). It was also found that the inactivation of HMG-CR was triggered by the conversion of cholesterol to 27-OHC (Lange et al., 2008). These studies are consistent with a modulatory role for 27-OHC. Down-regulated mRNA and protein levels of SREBP-1a, HMG-CR and LDLR in C6 cells after treatment with 27-OHC in our results indicate that 27-OHC may inhibit cholesterol generation by modulating the expression and content of synthesis mediators and subsequently resulting in a decline in the cholesterol content in C6 glioma cells.

The effects of 27-OHC on the expression of several genes involved in cholesterol transport in C6 glioma cells were also investigated. ABCA1 is a critical protein that regulates cholesterol efflux from cells and plays an important role in cholesterol metabolism (Gu et al., 2013). ApoE is a glycoprotein that is secreted by glial cells and forms part of a lipoprotein particle that transports cholesterol into neurons. PPAR-γ and LXR-α are important nuclear receptors that play crucial roles in cholesterol homeostasis and implicated in the activation of ABCA1and ApoE. Some evidence also supports LXR-α as a target gene of PPAR-γ that directly regulates ABCA1 expression (Xu et al., 2013). Previous studies have shown that treatment of primary human neurons with 27-OHC resulted in significant increase in ABCA1 mRNA and cellular levels of ApoE protein and mRNA (Kim et al., 2009). Additionally, 27-OHC was a potent partial agonist of LXR-α (Fu et al., 2001). In the present study, we detected that 27-OHC significantly enhanced the expression of PPAR-γ, LXR-α, ABCA1and ApoE in C6 cells, which indicates that 27-OHC might also promote cholesterol efflux in astrocytes by enhancing ABCA1, ApoE expression through activation of PPAR-γ/LXR-α pathway. These data further supported that 27-OHC may accelerate the cholesterol transport in C6 cells.

In our study, the rate of the apoptosis and viability of C6 glioma cells treated with 27-OHC is respectively higher and lower than that of control group. Individual astrocytes require large amounts of membrane and hence have a high demand for cholesterol (Pfrieger and Ungerer, 2011). Free cholesterol is essential for cellular viability. Michikawa et al. have found that inhibition of cholesterol production induces neuronal cell death (Michikawa and Yanagisawa, 1999). In addition, Marz et al. reported that treatment of astrocytes with statins, potent inhibitors of rate limiting enzyme for cholesterol biosynthesis, induced apoptosis (Marz et al., 2007). Cellular cholesterol homeostasis is crucial to various cellular functions and lack of cholesterol may also result in an impairment of glial cells (Guizzetti et al., 2007). Therefore, the significantly decreased viability and increased apoptosis of C6 cells induced by high concentration of 27-OHC may be explained by the observations that 27-OHC could alter cholesterol homeostasis and that such effects may be involved in its neurotoxicity. In line with this in vitro study, providing 27-OHC in vivo results in the same overall changes in brain cholesterol synthesis and trafficking as well as impaired cognition (Zhang et al., 2015).

Large content of free cholesterol is a common feature that astrocytes share with macrophages (Abildayeva et al., 2006) and macrophages are of great importance in normal and pathological cholesterol metabolism. As we have known in macrophages, cholesterol efflux pathways are pivotal because macrophages cannot limit the uptake of cholesterol from endogenous or exogenous sources (Zhao et al., 2010). Harmful buildup of cholesterol in macrophages is normally resisted by activating transport processes, whereby cholesterol is delivered to 27-OHC. It stimulates LXR-mediated transcription of ABCA1 and plays a key role in the efflux of excess cholesterol (Korytowski et al., 2015). Meanwhile, cholesterol excess, ultimately leading to increased oxysterols, stimulates SREBP-1c synthesis through the LXR-dependent mechanism, resulting in the elevated plasma triglycerides (Wojcicka et al., 2007). However, it should be noted that LXRs target genes include SREBP-1c, but not SREBP-1a (Wang et al., 2008). Thus, an impaired synthesis of cholesterol and enhanced cholesterol efflux, down-regulation of SREBP-1a and up-regulation of LXRα, were also reported as a consequence of 27-OHC treatment in C6 cells in our study. This can be reconciled with the fact that oxysterols, as naturally occurring ligands for the LXRs, regulate genes which modulate intacellular cholesterol through increased efflux via ABCA1 and storage as fatty acid via SREBP-1c.

5. Conclusion

In summary, our study demonstrates for the first time that 27-OHC is deleterious to C6 glioma cells by increasing apoptosis and reducing viability of the cells and more importantly disrupting the metabolism of cholesterol. Mechanistically, 27-OHC may inhibit cholesterol synthetic enzymes and metabolites, and activate cholesterol efflux, consequently disrupting cholesterol homeostasis. Taken together, 27-OHC may contribute to the cholesterol dysreguation and pathogenesis of neurological syndromes, thereby representing the link between hypercholesterolemia and neurodegenerative diseases.

Conflict of interest

The authors declare that there are no conflict of interest.

Acknowledgment

The research was supported by the State Key Program of the National Natural Science Foundation of China (Grant No. 81330065 and 81673149).

References

Abildayeva, K., Jansen, P.J., et al., 2006. 24(*S*)-hydroxycholesterol participates in a liver X receptor-controlled pathway in astrocytes that regulates apolipoprotein E-mediated cholesterol efflux. J. Biol. Chem. 281, 12799–12808.

Axelson, M., Larsson, O., 1995. Low density lipoprotein (LDL) cholesterol is converted to 27-hydroxycholesterol in human fibroblasts. Evidence that 27-

hydroxycholesterol can be an important intracellular mediator between LDL and the suppression of cholesterol production. J. Biol. Chem. 270, 15102–15110.
Bellosta, S., Corsini, A., et al., 1993. 27-Hydroxycholesterol modulation of low density lipoprotein metabolism in cultured human hepatic and extrahepatic cells. FEBS Lett. 332, 115–118.
Bjorkhem, I., Cedazo-Minguez, A., et al., 2009. Oxysterols and neurodegenerative diseases. Mol. Aspects Med. 30, 171–179.
Brown, A.J., Jessup, W., 1999. Oxysterols and atherosclerosis. Atherosclerosis 142, 1–28.
Di Paolo, G., Kim, T.W., 2011. Linking lipids to Alzheimer's disease: cholesterol and beyond. Nat. Rev. Neurosci. 12, 284–296.
Eberle, D., Hegarty, B., et al., 2004. SREBP transcription factors: master regulators of lipid homeostasis. Biochimie 86, 839–848.
Fu, X., Menke, J.G., et al., 2001. 27-hydroxycholesterol is an endogenous ligand for liver X receptor in cholesterol-loaded cells. J. Biol. Chem. 276, 38378–38387.
Gamba, P., Testa, G., et al., 2012. The link between altered cholesterol metabolism and Alzheimer's disease. Ann. N. Y. Acad. Sci. 1259, 54–64.
Gu, H.M., Li, G., et al., 2013. Characterization of palmitoylation of ATP binding cassette transporter G1: effect on protein trafficking and function. Biochim. Biophys. Acta 1831, 1067–1078.
Guizzetti, M., Chen, J., et al., 2007. Ethanol induces cholesterol efflux and up-regulates ATP-binding cassette cholesterol transporters in fetal astrocytes. J. Biol. Chem. 282, 18740–18749.
Heverin, M., Bogdanovic, N., et al., 2004. Changes in the levels of cerebral and extracerebral sterols in the brain of patients with Alzheimer's disease. J. Lipid Res. 45, 186–193.
Heverin, M., Meaney, S., et al., 2005. Crossing the barrier: net flux of 27-hydroxycholesterol into the human brain. J. Lipid Res. 46, 1047–1052.
Horton, J.D., Goldstein, J.L., et al., 2002. SREBPs: activators of the complete program of cholesterol and fatty acid synthesis in the liver. J. Clin. Invest. 109, 1125–1131.
Hughes, T.M., Rosano, C., et al., 2013. Brain cholesterol metabolism, oxysterols, and dementia. J. Alzheimers Dis. 33, 891–911.
Iuliano, L., Crick, P.J., et al., 2015. Cholesterol metabolites exported from human brain. Steroids 99, 189–193.
Javitt, N.B., 2007. Oxysterols: functional significance in fetal development and the maintenance of normal retinal function. Curr. Opin. Lipidol. 18, 283–288.
Kim, W.S., Chan, S.L., et al., 2009. Impact of 27-hydroxycholesterol on amyloid-beta peptide production and ATP-binding cassette transporter expression in primary human neurons. J. Alzheimers Dis. 16, 121–131.
Kivipelto, M., Helkala, E.L., et al, 1, 2001. Midlife vascular risk factors and late-life mild cognitive impairment: a population-based study. Neurology 56, 1683–1689.
Korytowski, W., Wawak, K., et al., 2015. Impairment of macrophage cholesterol efflux by cholesterol hydroperoxide trafficking: implications for atherogenesis under oxidative stress. Arterioscler. Thromb. Vasc. Biol. 35, 2104–2113.
Lange, Y., Ory, D.S., et al., 2008. Effectors of rapid homeostatic responses of endoplasmic reticulum cholesterol and 3-hydroxy-3-methylglutaryl-CoA reductase. J. Biol. Chem. 283, 1445–1455.
Leoni, V., Caccia, C., 2013. Potential diagnostic applications of side chain oxysterols analysis in plasma and cerebrospinal fluid. Biochem. Pharmacol. 86, 26–36.
Ma, W.W., Li, C.Q., et al., 2015. The oxysterol 27-hydroxycholesterol increases oxidative stress and regulate Nrf2 signaling pathway in astrocyte cells. Neurochem. Res. 40, 758–766.
Marwarha, G., Ghribi, O., 2014. Does the oxysterol 27-hydroxycholesterol underlie Alzheimer's disease-Parkinson's disease overlap? Exp. Gerontol..
Marz, P., Otten, U., et al., 2007. Statins induce differentiation and cell death in neurons and astroglia. Glia 55, 1–12.
Michikawa, M., Yanagisawa, K., 1999. Inhibition of cholesterol production but not of nonsterol isoprenoid products induces neuronal cell death. J. Neurochem. 72, 2278–2285.
Nicholson, A.M., Ferreira, A., 2010. Cholesterol and neuronal susceptibility to beta-amyloid toxicity. Cognit. Sci. (Hauppauge) 5, 35–56.
Pfrieger, F.W., Ungerer, N., 2011. Cholesterol metabolism in neurons and astrocytes. Prog. Lipid Res. 50, 357–371.
Pfrieger, F.W., 2003. Outsourcing in the brain: do neurons depend on cholesterol delivery by astrocytes? Bioessays 25, 72–78.
Prasanthi, J.R., Huls, A., et al., 2009. Differential effects of 24-hydroxycholesterol and 27-hydroxycholesterol on beta-amyloid precursor protein levels and processing in human neuroblastoma SH-SY5Y cells. Mol. Neurodegener. 4, 1.
Refolo, L.M., Malester, B., et al., 2000. Hypercholesterolemia accelerates the Alzheimer's amyloid pathology in a transgenic mouse model. Neurobiol. Dis. 7, 321–331.
Saeed, A., Floris, F., et al., 2014. 7alpha-hydroxy-3-oxo-4-cholestenoic acid in cerebrospinal fluid reflects the integrity of the blood-brain barrier. J. Lipid Res. 55, 313–318.
Solomon, A., Kivipelto, M., et al., 2009. Midlife serum cholesterol and increased risk of Alzheimer's and vascular dementia three decades later. Dement. Geriatr. Cognit. Disord. 28, 75–80.
Wang, Y., Muneton, S., et al., 2008. The effect of 24S-hydroxycholesterol on cholesterol homeostasis in neurons: quantitative changes to the cortical neuron proteome. J. Proteome Res. 7, 1606–1614.
Wang, H.L., Wang, Y.Y., et al., 2016. Cholesterol, 24-hydroxycholesterol, and 27-hydroxycholesterol as surrogate biomarkers in cerebrospinal fluid in mild cognitive impairment and Alzheimer's disease: a meta-analysis. J. Alzheimers Dis. 51, 45–55.
Wojcicka, G., Jamroz-Wisniewska, A., et al., 2007. Liver X receptors (LXRs) part I: structure, function, regulation of activity, and role in lipid metabolism. Postepy Hig. Med. Dosw. (Online) 61, 736–759.
Xu, X., Li, Q., et al., 2013. Arctigenin promotes cholesterol efflux from THP-1 macrophages through PPAR-gamma/LXR-alpha signaling pathway. Biochem. Biophys. Res. Commun. 441, 321–326.
Zhang, D.D., Yu, H.L., et al., 2015. 27-Hydroxycholesterol contributes to disruptive effects on learning and memory by modulating cholesterol metabolism in the rat brain. Neuroscience 300, 163–173.
Zhao, Y., Van Berkel, T.J., et al., 2010. Relative roles of various efflux pathways in net cholesterol efflux from macrophage foam cells in atherosclerotic lesions. Curr. Opin. Lipidol. 21, 441–453.